

RESEARCH

Open Access



Genome-wide gene network uncover temporal and spatial changes of genes in auxin homeostasis during fruit development in strawberry (*F. × ananassa*)

Yoon Jeong Jang¹ , Taehoon Kim⁴ , Makou Lin³ , Jeongim Kim^{2,3} , Kevin Begcy^{3,4} , Zhongchi Liu⁵ and Seonghee Lee^{1*}

Abstract

Background The plant hormone auxin plays a crucial role in regulating important functions in strawberry fruit development. Although a few studies have described the complex auxin biosynthetic and signaling pathway in wild diploid strawberry (*Fragaria vesca*), the molecular mechanisms underlying auxin biosynthesis and crosstalk in octoploid strawberry fruit development are not fully characterized. To address this knowledge gap, comprehensive transcriptomic analyses were conducted at different stages of fruit development and compared between the achene and receptacle to identify developmentally regulated auxin biosynthetic genes and transcription factors during the fruit ripening process. Similar to wild diploid strawberry, octoploid strawberry accumulates high levels of auxin in achene compared to receptacle.

Results Genes involved in auxin biosynthesis and conjugation, such as Tryptophan Aminotransferase of Arabidopsis (TAAs), YUCCA (YUCs), and Gretchen Hagen 3 (GH3s), were found to be primarily expressed in the achene, with low expression in the receptacle. Interestingly, several genes involved in auxin transport and signaling like Pin-Formed (PINs), Auxin/Indole-3-Acetic Acid Proteins (Aux/IAAs), Transport Inhibitor Response 1 / Auxin-Signaling F-Box (TIR/AFBs) and Auxin Response Factor (ARFs) were more abundantly expressed in the receptacle. Moreover, by examining DEGs and their transcriptional profiles across all six developmental stages, we identified key auxin-related genes co-clustered with transcription factors from the NAM-ATAF1,2-CUC2/WRKYGQK motif (NAC/WYKY), Heat Shock Transcription Factor and Heat Shock Proteins (HSF/HSF), APETALA2/Ethylene Responsive Factor (AP2/ERF) and MYB transcription factor groups.

Conclusions These results elucidate the complex regulatory network of auxin biosynthesis and its intricate crosstalk within the achene and receptacle, enriching our understanding of fruit development in octoploid strawberries.

Keywords Auxin, Strawberry fruit, Plant hormone, Achene, Receptacle, Transcriptomics

*Correspondence:

Seonghee Lee
seonghee105@ufl.edu

Full list of author information is available at the end of the article



© The Author(s) 2024. **Open Access** This article is licensed under a Creative Commons Attribution 4.0 International License, which permits use, sharing, adaptation, distribution and reproduction in any medium or format, as long as you give appropriate credit to the original author(s) and the source, provide a link to the Creative Commons licence, and indicate if changes were made. The images or other third party material in this article are included in the article's Creative Commons licence, unless indicated otherwise in a credit line to the material. If material is not included in the article's Creative Commons licence and your intended use is not permitted by statutory regulation or exceeds the permitted use, you will need to obtain permission directly from the copyright holder. To view a copy of this licence, visit <http://creativecommons.org/licenses/by/4.0/>.

Introduction

The garden strawberry (*Fragaria* × *ananassa*), an allo-octoploid fruit crop ($2n=8x=56$), originated from the hybridization of two wild octoploid species, *F. chiloensis* subsp. *chiloensis* and *F. virginiana* subsp. *virginiana*. It presents a genomic complexity with four subgenomes derived from different diploid progenitors: *F. vesca*, *F. iinumae*, *F. nipponica*, and *F. viridis*, as proposed by previous studies, [1, 2]. Strawberries belonging to the Rosaceae family, are distinguished by their unique achenetum fruit architecture, where a single flower produces many achenes (fertilized ovaries), contrasting with the fleshy fruits of apples, peaches, and pears [3, 4]. This distinction in fruit type, notably in strawberries and raspberries as aggregate fruits significantly influences morphology, production, storage, and distribution of their unique fruits [3–5]. Fertilization-induced fruit development in strawberries is of interest due to their unique flower and fruit structure. The strawberry fruit consists of numerous individual achenes embedded in a fleshy receptacle [6]. It is worth noting that what is commonly referred to as the fleshy fruit of a strawberry is actually a pseudocarp derived from the enlarged receptacle, while the true fruit (achene) is located on the epidermal layer [7, 8]. The fruit set is the primary and crucial point for fruit growth in plants, and typically triggered by positive signals generated during the process of fertilization [9]. Fruit set can arise from different parts of the flower, such as the ovary in tomato (*Solanum lycopersicum*), receptacle in strawberry, and accessory part of hypanthium in apple (*Malus domestica*) [10–13]. In many plant species, the process of fruit set is largely dependent on the occurrence of fertilization. After successful pollination and fertilization, a series of physiological and molecular changes occur, ultimately leading to fruit development [14]. Flowers that do not undergo pollination and fertilization typically wither and fall off.

Plant growth hormones such as auxin, gibberellin, abscisic acid (ABA), and cytokinin, are essential regulators of strawberry fruit development. These hormones regulate diverse biological processes, including promoting growth, increasing fruit size, and enhancing fruit set and yield [15–17]. Particularly, auxin is essential for fruit development, as it regulates cell division and differentiation in the receptacle, and its levels are dramatically regulated during fruit growth and ripening [18]. Although auxins such as indole-3-acetic acid (IAA) and phenylacetic acid (PAA) are crucial for plant growth and development, the complex biosynthetic pathways and enzyme redundancy within these pathways have hindered their complete understanding in plants, ranging from the model plant *Arabidopsis* to the crop model for fruit development [19, 20]. Previous studies have

demonstrated that auxin transport in the achene ceased during the late stages of mid-green fruit development to the ripening process of strawberry. This leads to a decrease in auxin levels in the receptacle and the subsequent ripening process [21]. Furthermore, prior studies also reported that removal of the achene from the receptacle after pollination inhibits fruit enlargement, while exogenous application of auxin promotes receptacle growth in the absence of achene [22–24]. Consequently, the achenes play a key role in auxin production needed to accelerate receptacle development [23]. Despite numerous studies on the complex biosynthesis and signaling pathways of auxin in wild diploid strawberries (*F. vesca*), the fundamental molecular mechanisms of auxin biosynthesis in octoploid strawberries, based on the high-quality haplotype-phased reference genome, have not yet been elucidated. Additionally, the intricacies of the differential gene expressions between achenes and the receptacle during fruit development in octoploid strawberries still need to be characterized.

In *Arabidopsis*, IAA biosynthesis occurs mainly through the two-step biosynthetic pathways catalyzed by the amino transferases (Tryptophan aminotransferase of *Arabidopsis* (TAA) and TAA-related (TAR)), and monooxygenases belonging to the YUCCA (YUC) family that respectively convert Trp to Indole-3-pyruvic acid (IPyA) and IPyA to IAA [20, 25]. Homologs of TAA/TAR and YUC have been identified in strawberry and implicated in various developmental processes, including fruit development. Several transcriptome profiling studies with *F. vesca* have shown that the auxin biosynthetic genes such as *FvYUC* and *FvTAA*, are predominantly induced in the endosperm after fertilization. Specifically, *FvYUC5*, *FvYUC11*, and *FvTAR1* were primarily expressed in the achene, with low expression in the receptacle, and highly expressed in ghost (seedcoat + endosperm) and less so in the embryo and ovary wall [11]. It was also reported that *FvYUC4* and *FvTAR2* were more abundantly expressed in the embryo, indicating their potential roles in embryonic development, while *FvYUC10*, *FvGA20ox1*, *FvGA20ox2*, and *FvGA3ox1* were present across various fruit tissues, exhibiting minimal to no expression within embryos. The expression of most of these biosynthetic genes gradually increases from stage 1 (open flower) to stages 5 (big green), likely due to the effect of fertilization [11]. Additionally, it was discovered that the wild strawberry *F. vesca* possesses nine genetic loci of *YUCs* genes, eight of which encode functional proteins. Specifically, the overexpression of *FvYUC6* exhibited delayed flowering and male sterility in transgenic strawberry plants. Plants with reduced expression of *FvYUC6* through RNAi demonstrated alterations in

floral organ structure and root development [26]. In the transcriptome analysis of cultivated strawberries, two *YUC* genes, *FaYUC1* and *FaYUC2* (homologous to *AtYUC6* and *AtYUC4*, respectively), were identified. *FaYUC1* and *FaYUC2* are highly expressed in the large green fruit stage. Notably, the expression level of *FaYUC2* is much higher compared to *FaYUC1* [27]. During late-stage fruit development, *FaYUC2*, *FaTAR2*, and *FaTAA1* were highly expressed in fruit receptacle [18, 28].

Research on the plant hormone auxin, especially its perception and transcriptional regulation, is a critical aspect of plant phytohormone studies. Previous studies have identified auxin receptors, including the F-box protein Transport Inhibitor Response 1 (TIR1), which facilitates the degradation of Auxin/Indole-3-Acetic Acid (Aux/IAA) transcriptional repressors [29]. At low auxin levels, Aux/IAA proteins act as repressors for expressing target genes like Auxin Response Factors (ARF). However, when auxin levels increase, Aux/IAA proteins are degraded by the 26S proteasome, leading to release ARFs to activate auxin responses [30]. In *F. vesca*, studies on Aux/IAA and ARF genes suggest that the perception and transcriptional regulation of auxin involve 21 *FvAux/IAAs* and 19 *FvARFs* genes [11]. Furthermore, the expression of 19 *FaAux/IAA* genes was detected in the receptacle of cultivated strawberries. Most of these genes exhibited a consistent decrease in expression as the fruit transitioned from green to red stages. However, *FaAux/IAA14b* and *FaAux/IAA11* showed maximum expression during the turning red stage, followed by a decrease in the red stage. For *FaARF* genes, while most showed low levels of expression from green to red stages, *FaARF6a* was notably more highly expressed during this transition compared to other *FaARF* genes [28]. Despite the large amount of evidence, a detailed molecular mechanism controlling auxin perception and gene regulation in octoploid strawberries, particularly within specific tissues such as achenes and receptacles remains unclear.

In this study, a genome-wide transcriptome analysis was performed with a recent complete haplotype-phased octoploid strawberry reference genome of 'Royal Royce' (FaRR1) at various fruit developmental stages [31]. Our results showed specific genes differentially expressed in receptacle and achenes during fruit development in octoploid strawberry. This deep transcriptome profiling identified genes involved in auxin biosynthetic signaling and metabolism pathways in strawberry. Moreover, our study identified novel transcription factors intricately linked to the auxin signaling network, marking a significant advancement in understanding the complex interplay between achenes and receptacles during the fruit development phase.

Results

Accumulation of IAA in achene and receptacle during fruit development

To investigate the developmental variations in IAA content of achenes and receptacles during fruit maturation, fruits of six different developmental stages were characterized. Stage 1; Small Green (SG), Stage 2; Medium Green (MG), Stage 3; Large Green (LG), Stage 4; White (W), Stage 5; Turning Red (TR), and Stage 6; Red (R) (Fig. 1A). For each developmental stage, achenes and receptacles of individual fruits were separated and the concentration of IAA was quantified. The IAA content was consistently higher in achenes of all six stages, compared to the IAA detected in receptacles (Fig. 1A and B). The highest IAA content was observed in the achenes of the SG and MG stage (approximately 4,000 – 7,000 pmol/g FW). The concentration of IAA in achenes decreased as the fruit matured and showed the lowest level of IAA at stage R (approximately 1000 – 2000 pmol/g FW) (Fig. 1B). Based on one-way ANOVA Tukey's test, achenes at stages SG and MG contained significantly greater IAA content compared to the R stage ($P < 0.05$). In contrast, receptacles exhibited significantly reduced IAA content in all stages of fruit development, but the highest IAA level was seen in the SG stage (approximately 50–110 pmol/g FW). A rapid decrease in IAA content at the MG stage of receptacles was observed, with concentrations dropping below 20 pmol/g FW (Fig. 1C). This reduction in IAA content in the receptacles after the SG stage persisted to maturity at the R stage.

Comparative transcriptome profiling analysis

between achene and receptacle during fruit development

To investigate the transcriptional changes during achene and receptacle development (SG, MG, LG, W, TR, and R) related to auxin homeostasis an RNA sequencing approach was used. Sequencing reads were mapped to the octoploid strawberry reference genome, cv. 'Royal Royce' (FaRR1) (www.rosaceae.org), resulting in a high average mapping rate of 95.6% for achene samples and 95.3% for receptacle samples (Table S1 and S2). Principal component analysis (PCA) was performed for the data quality assessment and exploratory analysis. Principal component 1 (PC1) accounted for 70% of the total variance, clearly delineating between achene and receptacle samples. Furthermore, principal component 2 (PC2) accounted for 22% of the total variance, distinguishing between the early and late stages of development. The PCA results suggest that the differences between achene and receptacle samples may reveal significant distinctions in the transcriptomes of these tissues across various stages of development

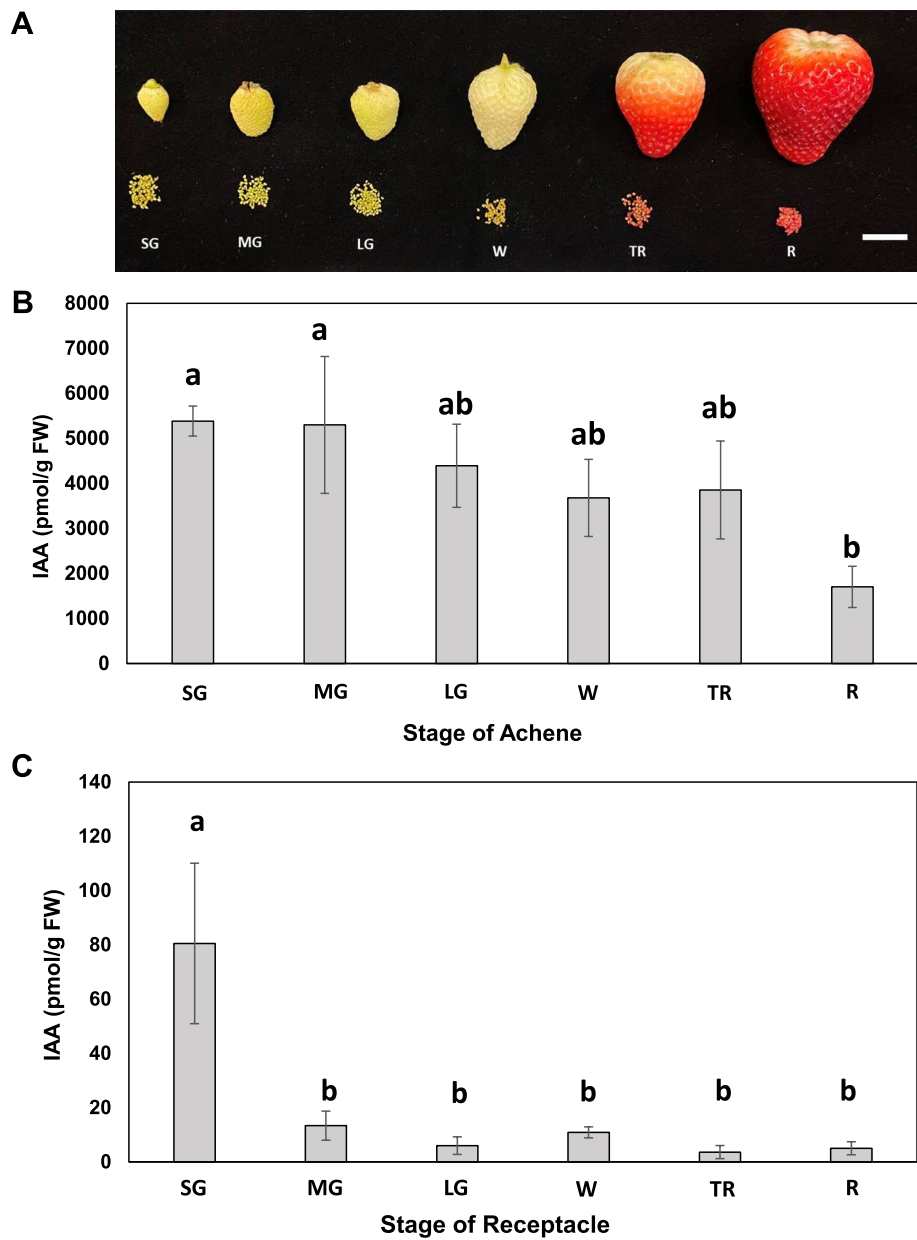


Fig. 1 IAA levels in strawberry achene and receptacle during fruit development. **A** Attached and detached achene and receptacle developmental stages of cultivar ‘Florida Brilliance’ (*Fragaria × ananassa* Duch). Stage 1; Small Green (SG), Stage 2; Medium Green (MG), Stage 3; Large Green (LG), Stage 4; White (W), Stage 5; Turning Red (TR), and Stage 6; Red (R). Scale bar: 2 cm. IAA contents in **B** achenes and **C** receptacles. Statistical analysis was conducted using one-way ANOVA Tukey’s test ($P < 0.05$). Different letters indicate significant differences in the amount of free IAA. Mean and standard deviation are shown ($n = 3$)

(Supplemental Fig. 1). To identify differentially expressed transcripts between achene and receptacle, we performed DESeq2 analysis using a significance cut-off $\text{padj} < 0.05$. The larger number of DEGs was identified in the comparison between achene and receptacle at the MG stage (32,686 DEGs total; 17,608 up-regulated and 15,078 down-regulated). In contrast, the comparison between achene and receptacle at the R stage yielded the smallest number of DEGs, totaling 7,131 DEGs from which 6,217 were up-regulated and 914 were down-regulated (Fig. 2A, Supplemental Fig. 2 and Supplemental Table 3). Venn diagrams were generated for pairwise comparisons between achene and receptacle at each stage (SG, MG, LG, W, TR, and R). A total of 2,892 genes commonly expressed across

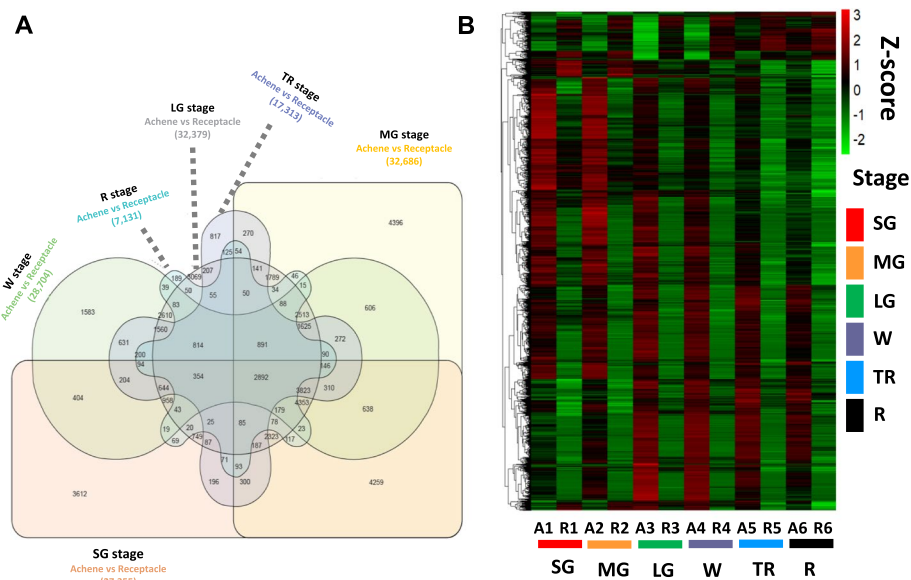


Fig. 2 Transcriptional changes across six stages of fruit development in achene and receptacle tissues. **A** Venn diagram displaying unique and overlapping sets of 2,892 DEGs identified in achene and receptacle tissues, $\text{padj} < 0.05$. **B** Heatmap analysis of 2,892 overlapping DEGs. Gene expression values are shown as Z-score, $\text{padj} < 0.05$. Developmental stages are color coded. Small Green (SG) in red. Medium Green (MG) in yellow. Large Green (LG) in green. White (W) in purple. Turning Red (TR) in blue and Red (R) stage in black

all stages of fruits were identified and further focused on analyzing their potential role in key metabolism, transport, signal, and response gene expression specific to each subgenome level (Fig. 2). To narrow down and analyze the transcription factors commonly involved, we also utilized this common 2,892 DEGs for the GO analysis. Moreover, stage-specific analyses revealed that 3,612, 4,396, 3,069, 1,583, 817, and 189 genes were uniquely expressed at SG, MG, LG, W, TR and R stages, respectively (Fig. 2A). Intriguingly, our findings reveal a notable decrease in the number of differentially expressed genes, particularly during the later developmental stages, including the W, TR, and R stages. Our results also showed a significant increase in the expression levels of achene-specific transcripts across the different fruit developmental stages. Additionally, the expression patterns of achene or receptacle-specific genes varied throughout different developmental stages (Fig. 2B). These observations highlight the substantial expression of achene-specific transcripts during fruit maturation. The observed variation in differentially gene expression patterns between achenes and receptacles during fruit maturation can be attributed to their distinct tissue compositions. Achenes, as more complex organs consisting of the embryo, endosperm, and seed coat, naturally display greater complexity and a higher number of differentially expressed genes. Conversely, the receptacle, a simpler organ composed of cortex and

pith, shows less variability in gene expression due to its more uniform tissue structure.

Dynamic differential gene expression in achene and receptacle during fruit development

To elucidate the functional dynamics of gene expression between achene and receptacle tissues across six developmental stages, we conducted Gene Ontology (GO) and Kyoto Encyclopedia of Genes and Genomes (KEGG) pathway enrichment analyses using the ShinyGO web tool. We used a total of 2,892 DEGs identified across all different developmental stages of achene and receptacle ($\text{padj} < 0.05$) and subjected them to GO analysis to determine their associated Biological Process (BP), Cell Components (CC), and Molecular Functions (MF) associated with each gene (Fig. 3 and Supplemental Table 4). Within the BP category, DEGs between achene and receptacle common to each of the six developmental stages were primarily involved in pathways including the phenylpropanoid metabolic process, post-embryonic development, phenylpropanoid biosynthesis, as well as lignin metabolism and biosynthesis. Of particular note, we observed a common expression pattern of genes related to the response to hormone (GO:0009725) across all six stages (Fig. 3, Supplemental Table 4). Additionally, in the CC category, the DEGs were found to relate to cellular components such as the vacuole, bounding membrane of

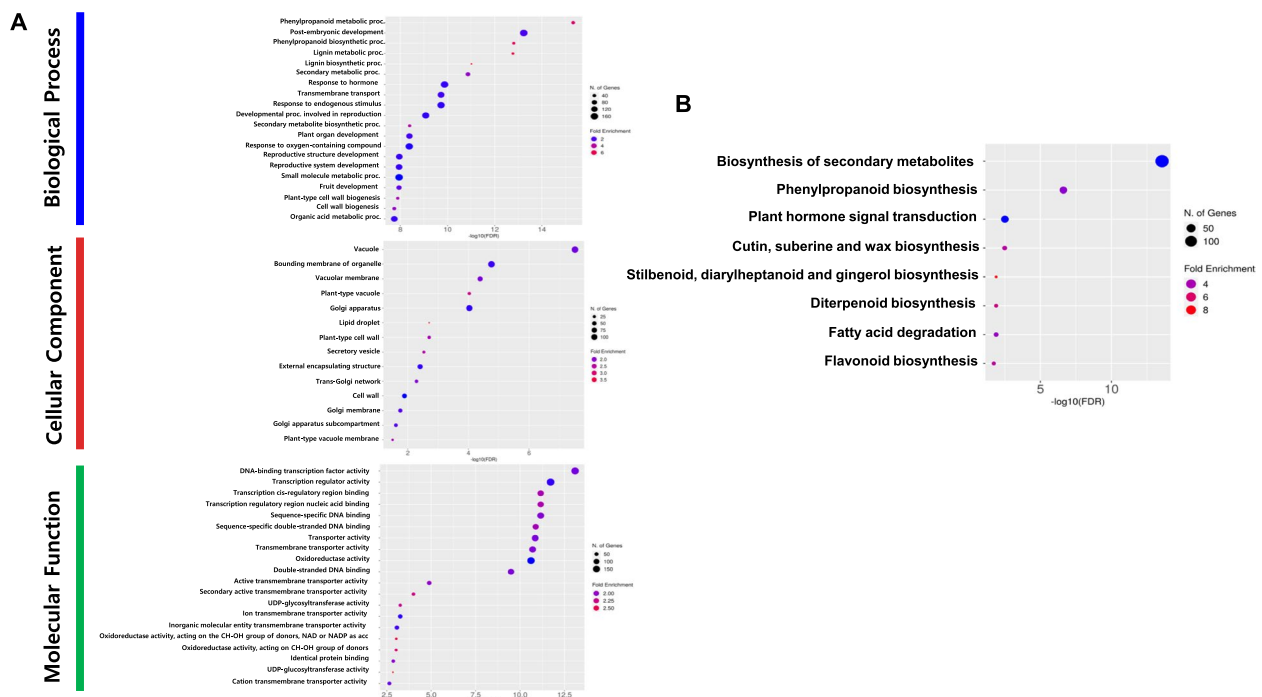
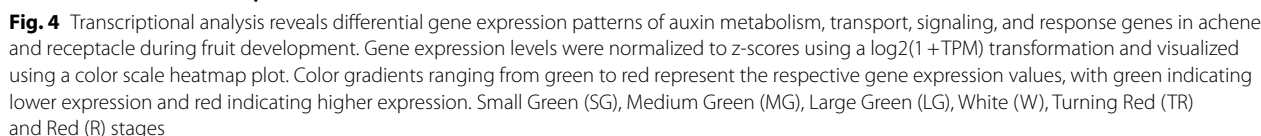


Fig. 3 GO and KEGG pathway enrichment analyses of differentially expressed genes in achene and receptacle. **A** Fold enrichment for GO biological process (BP), cellular component (CC) and Molecular function (MF). The x-axis indicates the $-\log_{10}$ FDR, and the y-axis shows the GO terms. Colors represent the degree of enrichment. **B** Bubble diagram highlights eight significant KEGG pathways, with circle sizes reflecting the number of DEG counts. Pathways with the highest significance ($FDR < 0.05$) are delineated within respective clusters

organelle, vacuolar membrane, plant-type vacuole, and Golgi apparatus, among others (Fig. 3, Supplemental Table 4). Interestingly, in the MF category, a significant enrichment of transcription factors and DNA-binding activities was observed, including DNA-binding transcription factor activity, transcription regulator activity, transcription cis-regulatory region binding, transcription regulatory region nucleic acid binding, and sequence-specific DNA binding (Fig. 3, Table S4). These findings suggest the presence of genes commonly expressed in both the achene and receptacle, and possibly linked to important functional mechanisms in the process of fruit development in octoploid strawberry. We also performed a KEGG pathway enrichment analysis on the 2,892 overlapped stage candidate DEGs identified. The primary signaling pathways associated with strawberry in the comparison between achene and receptacle include: Biosynthesis of secondary metabolites (139), Phenylpropanoid biosynthesis (31), Plant hormone signal transduction (32), Cutin, suberine and wax biosynthesis (9), stilbenoid, diarylheptanoid, and gingerol biosynthesis (4), Diterpenoid biosynthesis (6), Fatty acid degradation (9), and Flavonoid biosynthesis (6) (Fig. 3B and Supplemental Table 5).

Identification of genes involved in auxin homeostasis in achene and receptacle during fruit development of octoploid strawberry

The expression levels of genes associated with auxin homeostasis were determined in achene and receptacle, and a total of 181 genes were identified. We filtered these genes based on the criteria of $p_{adj} < 0.05$ and $TPM < 0.5$, resulting in the final selection of 159 auxin-related genes (Fig. 4, Supplemental Table 6). The TAAs and YUCs are essential components for the biosynthesis of the major natural auxin in plants, IAA. As the IPyA pathway mediated by TAAs and YUCs produces the majority of free IAA, the expression of TAAs and YUCs is indispensable for various essential developmental processes, including fruit development. In the octoploid strawberry ‘Royal Royce’, we identified TAA1 homoeologous gene copies located in the four subgenome of chromosome 4, *Fxa4Ag102498*, *Fxa4Bg102453*, *Fxa4Cg202161*, and *Fxa4Dg101990* (Fig. 4). Among these copies, we found that *Fxa4Bg102453*, *Fxa4Cg202161*, and *Fxa4Dg101990* had high expression levels at the SG stage of achenes. Moreover, we identified homoeologous gene copies of TAR1/2, including *Fxa5Ag200524*, *Fxa5Bg100503*, *Fxa5Cg200481*, and *Fxa5Dg200494*, respectively (Fig. 4). All four copies showed high



In addition, four *FaYUC* genes, *FaYUC2*, *FaYUC4*, *FaYUC10* and *FaYUC11*, were found in the octoploid strawberry. Protein analysis using the *FvYUC2* sequence from diploid strawberry showed high similarity with four homoeologous copies of *FaYUC2*, *Fxa1Ag100425*, *Fxa1Bg200419*, *Fxa1Cg100379*, and *Fxa1Dg200387* (Fig. 4). The gene expression result showed that only *Fxa1Cg100379* appears to be dominantly expressed at the LG stage at achene, while the expression of the other three copies is either absent or very low. For *FaYUC4*, interestingly, all four homoeologous copies of *Fxa2Ag102968*, *Fxa2Bg202798*, *Fxa2Cg201097*, and *Fxa2Dg202579* located in chromosome 2 are highly

Furthermore, we identified high expressions of *GH3* genes, which belong to one of the major auxin-responsive gene families. *FaGH3.1*, *FaGH3.5*, *FaGH3.6a*, *FaGH3.6b*, *FaGH3.9*, and *FaGH3.17* showed expression levels with LogFC values from 0.48 to 6.06 (average=2.4) at the

SG stage and from 0.57 to 7.97 (average=2.67) at the MG stage in achenes, respectively (Fig. 4, Supplemental Tables 3 and 6). It has been known that *GH3s* play crucial roles in auxin homeostasis through conjugating free auxin with amino acids [32]. We identified that the *FaGH3.5* homoeologous gene copies, *Fxa6Ag104259*, *Fxa6Bg103912*, *Fxa6Cg103796*, and *Fxa6Dg103714*, were highly expressed in the achene during the SG and MG stages. Interestingly, only one copy of *FaGH3.6* (*Fxa3Ag100357*) was highly expressed in receptacle during the SG and MG stages compared to the achene. Furthermore, *FaGH3.6a*, *FaGH3.6b*, *FaGH3.9*, and *FaGH3.17* showed predominantly high expression levels at the SG and MG stages of achene. Particularly, the three homoeologous copies of *FaGH3.6b*, *Fxa3Bg201817*, *Fxa3Cg101795*, and *Fxa3Dg201745*, showed high expression levels in the achene at the SG stage (Fig. 4).

To investigate the alternative auxin biosynthesis pathways in octoploid strawberries, we analyzed the expression levels of genes involved in known auxin synthetic pathways, such as the IPA, IAOx, and IAM pathways (Supplemental Fig. 3). Several genes related to alternative auxin biosynthesis were identified. Notably, the *FaAM11* gene family, which encodes amidase 1, is involved in converting IAM (Indole-3-Acetamide) to IAA (Indole-3-Acetic Acid). The heatmap shows variable expression levels of AM11 across different tissues, with predominant expression at the LG stage in the receptacle, indicating its active role in the IAM pathway. The genes CYP79A2/B2 and CYP79B3 (*Fxa3Ag100864*), part of the pathway converting tryptophan to IAOx (Indole-3-Acetaldoxime), exhibited high expression levels in specific red each achene and receptacle developmental stages, suggesting their involvement in the IAOx pathway.

For the PIN family genes, six homologs of PIN 1, 2, 4, 5, 8, and 10 were identified in *F. × ananassa* utilizing *F. vesca* as a query. Among them, *FaPIN1*, *FaPIN4*, *FaPIN5*, and *FaPIN8* exhibited stronger expression in the receptacle at SG than in achene at SG, but *FaPIN10* showed the opposite pattern. Homologs of AUX/LAX genes, including *AUX/LAX2*, *AUX/LAX3*, and *AUX/LAX4*, were identified in *F. × ananassa*. While *FaAUX/LAX2* exhibited high gene expression at MG of achene. *FaAUX/LAX4* showed stronger gene expression at SG and MG of achene compared to receptacle (Fig. 4). We also discovered nine *Aux/IAA* genes and 14 ARF gene family homologs in *F. × ananassa*. Among them, *FaAux/IAA26b* displayed differences in gene expression between achene and receptacle at MG. *FaAux/IAA27a* and *FaAux/IAA27b* showed slight differences in expression between achene and receptacle at SG and MG. Notably, at SG and MG, *FaARF3*, *FaARF6a*, *FaARF19a*, and *FaARF19b* gene families exhibited higher expression in receptacle

than in achene. However, *FaARF1b* displayed higher expression in achene from MG to W stage, and some genes including *FaARF16a*, *FaARF16b*, and *FaARF17a,c* showed higher expression in SG of achene compared to receptacle. Lastly, TIR1, AFB2, and AFB5 homologs were also identified in *F. × ananassa*. These auxin biosynthesis-related genes influence various aspects of *F. × ananassa* fruit effects, including growth, perception of auxin, and more, throughout the stages from early to late, suggesting their multifaceted impact on the fruit development of octoploid strawberry (Fig. 4).

Transcription factors involved in auxin biosynthesis signaling networks between achenes and receptacles during fruit development

To further understand auxin biosynthesis and transport between achene and receptacle, we used the entire list of DEG and clustered them across all six developmental stages based on their transcriptional expression. We identified four distinctive patterns of expression (Fig. 5, Table S7). Cluster 1 was formed by 1209 genes with increasing expression in achene having the highest expression at LG. Genes in cluster 1 have a low or no expression in the six receptacle developmental stages (Fig. 5A). Cluster 2 formed by 1229 genes showed a decreased expression from achene to receptacle in a developmental manner. The more advanced the developmental stage the lower the expression (Fig. 5A). Cluster 3 showed an opposite pattern as cluster 1, having lower expression in the achene and higher expression in the receptacle (Fig. 5A). Finally, cluster 4 formed by 177 genes, showed variable expression across developmental stages in achene and receptacles samples (Fig. 5A).

Since cluster 1 showed opposite developmental expression between achene and receptacle, we selected the entire set of genes identified in this cluster to conduct a correlation analysis to pinpoint transcription factors with shared expression profiles with genes involved in auxin biosynthesis and transport between achene and receptacle. A large portion of the strawberry genes are described as uncharacterized or unknown. Therefore, we removed them from the analysis. After removal of unrooted genes, the remaining genes were clustered using an edge confidence of at least 0.7. Our analysis yielded six main hubs containing transcription factors associated with auxin related genes (Fig. 5B). These transcription factor hubs were grouped into NAC/WYKR (blue), bZIP (black), heat shock transcription factor-HSF/HSPs (red), homeobox (orange), bHLH (brown), APETALA2/Ethylene Responsive Factor-AP2/ERF (purple), and MYB (green). Since we were interested in auxin biosynthesis and transport, we identified the auxin related genes (yellow) that clustered together with other transcription factors.

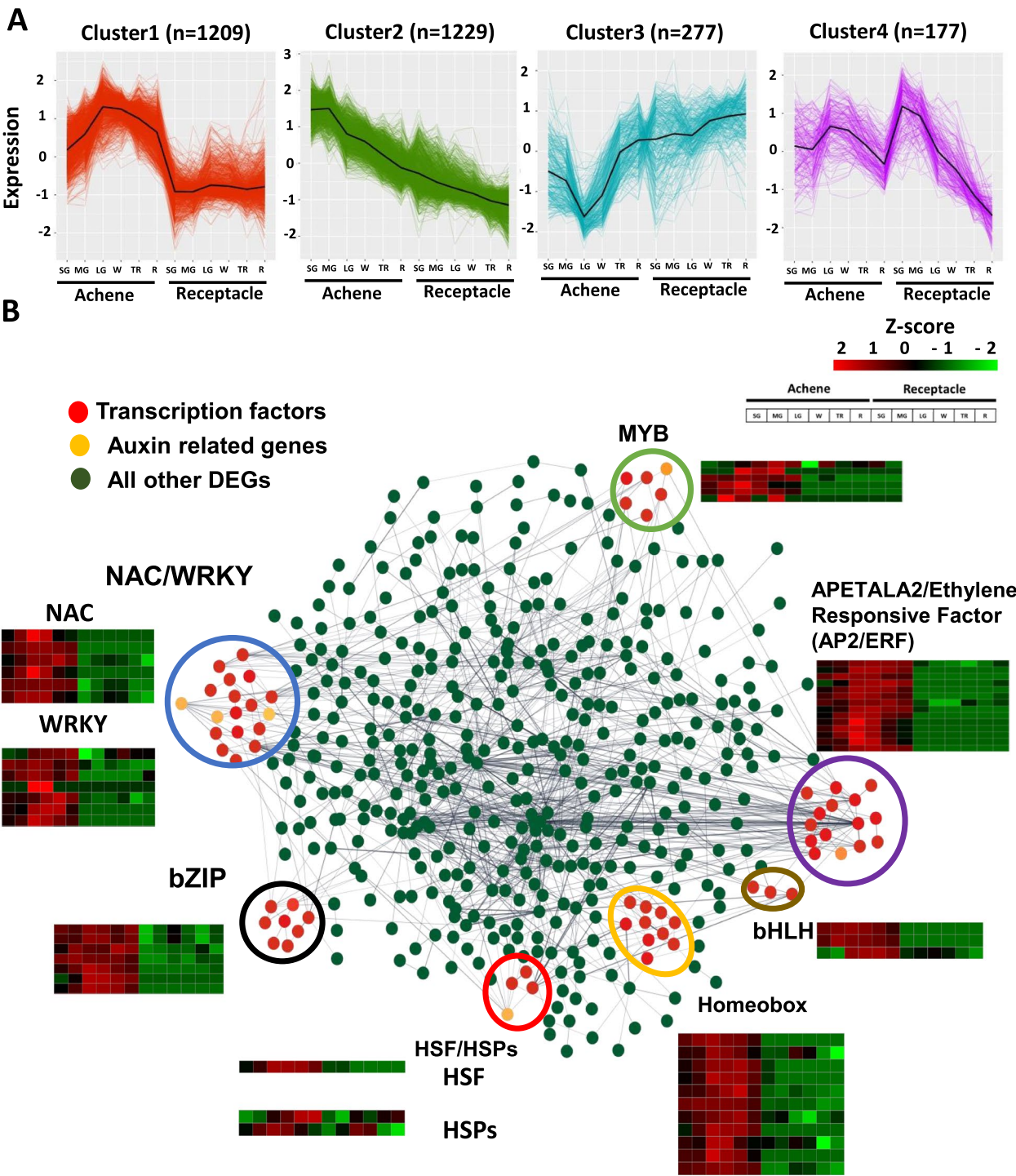


Fig. 5 Novel transcription factors involved in gene regulation between achenes and receptacles of strawberry fruits. **A** Clustering analysis including all differentially expressed genes. **B** Gene network analysis of differentially expressed genes between achenes and receptacles. Transcription factors are shown in red. Auxin related genes are shown in yellow. All other differentially expressed genes are shown in green. A threshold of 0.7 of edge confidence was used. A detailed list of the genes included in the gene interaction analysis can be found in Supporting Table S7

Interestingly, four of the seven transcription factor hubs identified in our analysis contained auxin-related genes. The *FaARF4* gene (*Fxa2Bg202325*) and the Auxin efflux carrier (*Fxa4Ag100605*), along with a DNA-binding pseudobarrel domain superfamily gene (*Fxa5Dg200932*, homologous to *FvARF11*), were found to cluster with the NAC/WRKY transcription factors. The ABC-2 type transporter gene (*Fxa6Ag100719*) was associated with the HSF/HSPs group, while *FaYUC11* (*Fxa4Bg101727*) and the B3 DNA binding domain gene (*Fxa7Cg101837*, homologous to *FvARF16c*) clustered with the AP2/ERF and MYB transcription factor hubs, respectively (Fig. 5B). To validate these findings, we performed qRT-PCR analysis on the auxin-related genes marked in yellow in Fig. 5B. This analysis confirmed that these genes were predominantly expressed in the achenes across all six developmental stages, as opposed to the receptacles (Supplemental Fig. 4).

Discussion

The plant hormone auxin plays a fundamental role in regulating cell expansion and cell division [33, 34]. Previous studies indicate that fruit development is intricately linked to achene growth, with the maturation of fleshy fruits being inhibited in the absence of achene. This repression is relieved when fertilized achenes release auxin signals to the ovary wall and receptacle [35]. In strawberries, achenes are considered the principal sites for auxin accumulation, playing a pivotal role in regulating auxin distribution across the entire fruit, thereby influencing its development [11, 21, 36]. Studies on auxin in wild diploid strawberry, *Fragaria vesca*, have shown that auxin increases both the width and length of the fruit during the early stages of fruit development, while gibberellic acid (GA), mainly promotes vertical growth [17].

Auxin dynamics in achene-derived auxin on receptacle growth and strawberry fruit development

Perkins-Veazie classified the ripening stages of strawberry fruit into four stages (green, white, pink, and red), with pink being reported as the turning point of ripening [8]. However, given that several previous studies have indicated the significant role of auxin synthesis and transport in the early developmental stages of strawberry growth, our research has not only divided the developmental process into six distinct stages, from early development to maturity but also separated achene and receptacle at each stage for hormone measurement and transcriptome analysis (Fig. 1). A previous study has reported a consistent reduction in IAA as the fruit transitions from the small green stage to the red stage, as shown in mixed tissue of achene and receptacle [37]. In our study, when analyzing

the auxin content separately in the achene and receptacle of octoploid strawberries, we observed a significantly higher concentration of auxin in the achene compared to the receptacle, as observed in Fig. 1. This finding agrees with the previous report that the receptacle enlargement would be associated with auxin in achenes. Our results corroborate those of Estrada-Johnson et al. (2017) and Gu et al. (2019), who observed elevated IAA levels in achenes compared to receptacles during fruit development. Our study, however, distinguishes itself by employing a high-quality reference genome to perform detailed tissue-specific analyses across six developmental stages in octoploid strawberries, whereas Estrada-Johnson et al. (2017) focused on only four stages. Moreover, while Gu et al. (2019) examined the transcriptome and auxin-related genes in diploid strawberries, our analysis extends to octoploid strawberry varieties, providing a more comprehensive understanding of auxin dynamics across different genomic complexities [28, 38]. One intriguing finding is the presence of approximately 50–110 pmol/g FW of IAA in the receptacles at the small green stage. This could support the result of temporal variations in auxin distribution, where auxin is synthesized within the achene in early stage of fruit development and possibly associated with the enlargement of receptacle in later stages. Although present at a lower concentration compared to the achene, the IAA in the receptacle would contribute to the coordination of fruit development, possibly regulating processes such as cell division and expansion. This could support the notion that even with a lower concentration of auxin, the receptacle serves as a receiver and transporter of IAA to modulate the growth and development of the strawberry fruit [6, 11, 39].

Exploring auxin metabolism, transport, signaling, and response pathways in achene and receptacle

To investigate the regulation of this phenomenon by specific genes, we conducted a genome-wide comprehensive analysis of the auxin-specific transcriptome in the achene and receptacle of octoploid strawberries using the recently developed high-quality haplotype-phased reference genome for octoploid strawberries [31]. We compared and analyzed the transcriptomes separately for the achene and receptacle at each developmental stage. According to previous research, strawberry fruit set is completed within two to four days after fertilization, and it has been shown that transcriptional regulation and signaling metabolic changes occur at fertilization. This pattern is consistent with our results (Fig. 1 and Fig. 4) [11]. To determine the collaborative action of gene families involved in the biosynthesis and transport of auxin, we conducted a DEG analysis using the criteria under $\text{padj} < 0.05$ to identify significantly differentially

expressed genes at each developmental stage. In this study, we examined the expressions of homologous genes previously studied, such as TAA, TAR, YUC, GH3, Aux/IAA, TIR/AFB, and ARF, and found that the genes related to auxin biosynthesis were highly expressed during SG or MG in the achene. In the diploid strawberry *F. vesca*, Gu et al. (2019) reported a comprehensive analysis of hormone levels and transcriptomes throughout fruit maturation stages. Their study specifically included transcriptome analysis of the receptacle, which revealed patterns similar to our findings in octoploid strawberry receptacle transcriptomes (Supplemental Fig. 5). Interestingly, the analysis in *F. vesca* showed low gene expression levels for auxin metabolism genes in the receptacle. Based on these observations, we propose that the primary site for auxin metabolism in both diploid and octoploid strawberry is the achene. Throughout the comprehensive analysis in this study, it was found that genes such as TAA1, TAR1/2, YUC4, and GH3.6b play a pivotal role in auxin biosynthesis primarily within the achene. TAA and TAR enzymes are responsible for converting Trp to IAA in the IPA pathway. In this pathway, Trp undergoes a reversible amino transfer reaction, catalyzed by TAA1/TARs enzymes, to form IPA [40]. Additionally, it is notable that one of the TAA genes, *FaTAA1/TAR1,2*, shows accumulated transcripts starting from the SG stage in the achene (Fig. 4). This pattern is similarly coordinated with findings by Elizabeth et al. 2017 [28], which also observed that TAA1 has the highest expression at the SG stage in the achene. Furthermore, TAR1/2 genes also displayed elevated expression levels from the SG stage to the MG stage. Interestingly, *FaYUC10* and *FaYUC11* show sustained expression in the achene from the SG to TR stages. Additionally, *FaYUC4* exhibits high expression levels during the MG stage across all four sub-genomes (2A, 2B, 2C, 2D). Notably, EMS mutants Y422 and Y1011, which carry mutations in the *FvYUC4* gene, display reduced leaf blade width and altered floral organs and fruit size due to the loss of function in the *yuc4* gene. Complementary experiments demonstrated that increasing YUC4 gene function restored normal leaf and fruit development. These findings collectively suggest that *FvYUC4* plays a crucial role in regulating auxin hormones, which are essential for the overall morphology of strawberry leaves, flowers, and fruits [41]. Previous studies have also reported the high expression of auxin-conjugating GH3 genes in ghost and ovary walls at the *F. vesca* [11]. Furthermore, the presence of IAA amide conjugates and highly abundant IAA-protein conjugates have been reported in the receptacle of strawberries [42, 43]. Our transcriptome data corroborate these findings, showing GH3.2 expression specifically in the receptacle. GH3 proteins are known to maintain auxin homeostasis by

converting active IAA into inactive conjugates [44]. This regulation ensures that auxin levels do not become excessively high, preventing negative effects on plant growth and development. GH3 enzymes act as part of a feedback mechanism in auxin signaling pathways. Elevated levels of IAA can induce the expression of GH3 genes, which then conjugate IAA to maintain balance. Thus, it is plausible that the auxin synthesized in the achene during the SG stage is partially maintained and transported, while the GH3-mediated regulation in the receptacle helps modulate the auxin levels, contributing to the observed decrease in auxin concentration in the receptacle at the MG stage. Additionally, the PIN gene family, essential for auxin efflux facilitation, markedly impacts auxin's directional flow owing to their unique intracellular localization [45, 46]. In octoploid strawberries, particularly during the SG stage, the expression of specific PIN genes (*FaPIN4*, *FaPIN5*, and *FaPIN8*) is substantially elevated in the receptacle compared to the achene. This reaffirms the coordination of achene and receptacle in fruit development.

One notable aspect to consider is that in many species, a multitude of Aux/IAA proteins modulate ARF-mediated transcription and offer extensive signaling interactions in various processes involving auxin [47]. Also, the Aux/IAA genes have the important role regulating fruit growth and negative regulating ripening of strawberry [39]. In this research, we discovered that gene copies within the Aux/IAA family, specifically *FaAux/IAA26a* (*Fxa2Ag103448*, *Fxa2Bg203233*, *Fxa2Cg200618*, *Fxa2Dg203024*), *FaAux/IAA27a* (*Fxa1Ag100497*, *Fxa1Bg200482*, *Fxa1Cg100463*, *Fxa1Dg200444*), and *FaAux/IAA27b* (*Fxa6Ag103081*, *Fxa6Bg102848*, *Fxa6Cg102729*, *Fxa6Dg102648*), alongside TIR/AFB genes such as *FaTIR1* (*Fxa2Ag102496*, *Fxa2Bg202336*, *Fxa2Cg203243*, *Fxa2Dg202184*), *FaAFB2* (*Fxa6Ag105135*), and *FaAFB5* (*Fxa5Ag203451*, *Fxa5Bg103235*, *Fxa5Cg202953*, *Fxa5Dg203023*), and ARF genes including *FaARF3* (*Fxa3Dg20069*, *Fxa3Cg100717*, *Fxa3Ag100785*), *FaARF6a* (*Fxa3Cg100416*, *Fxa3Ag100462*), *FaARF19a* (*Fxa1Cg100787*, *Fxa1Dg200710*), and *FaARF19b* (*Fxa4Ag100540*, *Fxa4Bg100521*, *Fxa4Cg200482*, *Fxa4Dg100445*), demonstrated notably higher expression levels in the receptacle than in the achene. This differential expression was particularly evident during the early developmental stages, from SG to LG, respectively. Although we lack in-vivo evidence to definitively link these morphological changes to gene expression, our analysis revealed distinct differences in the expression of auxin-related genes between these stages. Previous research has shown that treating strawberries with exogenous auxin, specifically NAA, leads to increased expression of *FaAUX/IAA* genes, which in turn delays fruit ripening [39]. Furthermore, studies in apple have

identified a strong association between the *ARF106* gene and fruit size through QTL mapping in various F1 progeny populations, particularly during cell division and expansion phases. Expression analysis across four developmental stages further confirmed that *ARF7* and *ARF106* genes are highly expressed during these critical phases of fruit growth [48]. Considering our transcriptome data, we observed that *FaAUX/IAA* and *FaARF* genes in the receptacle exhibit peak expression during the SG and MG stages. This pattern suggests a potential correlation between the differential expression of these genes and the observed differences in fruit size. Therefore, our findings imply that these genes may play a significant role in regulating fruit development and growth, possibly contributing to the variations in fruit size observed during these stages. This intricate network of interactions may stem from gene expression driven by specific TIR/AFB, Aux/IAA, and ARF transcription factors in response to auxin [49].

To further explore the alternative auxin pathways, we conducted a comparative analysis of auxin biosynthesis genes in achene and receptacle tissues at various developmental stages. Several genes involved in the IAM and IAOx pathways were identified. Notably, the *FaAMI* gene family, exhibited strong expression in the receptacle, starting from the MG stage and peaking at the LG stage. The AMI1 gene encodes indole-3-acetamide hydrolase, an enzyme in an alternative tryptophan-dependent auxin biosynthesis pathway using indole-3-acetamide as an intermediate. Similar findings have been reported in mature apple fruit, where TAA/TAR and YUCCA gene expression is minimal in mature apple fruit, while AMI genes, such as AMI1 and AMI101, show high expression levels, indicating the significance of the IAM pathway [50]. Certainly, seeds (achene) are likely sites for auxin biosynthesis during fruit development. However, data on the relevant pathways and genes remain limited. Research in various plant species demonstrates that TAA/TAR and YUCCA gene expression is high in seed tissues and correlates with auxin accumulation, suggesting that this pathway might also be predominant in fruits [51–55].

Characterizing auxin transcription factors in achene and receptacle

Our study specifically aimed to elucidate the transcription factors associated with the genes discovered during fruit development in octoploid strawberry. We focused on transcription factors that exhibit co-expression patterns with genes involved in auxin biosynthesis and transport within both achene and

receptacle tissues. Our study uncovered a fascinating interplay between auxin-related genes and major transcription factor hubs, including NAC/WRKY, HSF/HSPs, AP2/ERF, and MYB. Notably, the *FaARF4* gene (*Fxa2Bg202325*) and the Auxin efflux carrier gene (*Fxa4Ag100605*), along with a gene from the DNA-binding pseudobarrel domain superfamily (*Fxa5Dg200932*, homologous to *FvARF11*), were co-localized with NAC/WRKY transcription factors. In the study by Carrasco-Orellana et al. (2018) on *Fragaria chiloensis*, it was highlighted that multiple TFs play critical roles in regulating fruit ripening [56]. Specifically, the NAC family of transcription factors has been associated with cell wall remodeling processes during this developmental phase. Additionally, in silico analysis identified cis-regulatory elements within these genes that are responsive to hormones such as auxin and ABA. These elements, known as Secondary wall NAC binding elements (SNBE), suggest a coordinated regulatory mechanism involving these hormones in the modulation of fruit ripening and related physiological changes [56]. Additionally, *FaYUC11* (*Fxa4Bg101727*) was clustered with the AP2/ERF group, suggesting a regulatory synergy in auxin signaling pathways. Auxin is thought to indirectly facilitate fruit ripening by enhancing the transcription of various ethylene components, which subsequently results in ethylene-triggered ripening and fruit softening [57]. The B3 DNA binding domain gene (*Fxa7Cg101837*, homologous to *FvARF16c*) was found within the MYB transcription factor cluster. This collective data suggests potential transcription factors that may play a crucial role in regulating auxin biosynthesis and its transport dynamics between achene and receptacle during strawberry fruit ripening.

Conclusions

In our study provides comprehensive gene expression profiling specific at subgenome level of octoploid strawberries from early to late fruit developmental stages. This information highlights an important yet insufficiently explored area in the field of octoploid strawberry auxin research. Furthermore, identifying patterns of subgenome-specific gene expression would implicate pathways of auxin metabolites, as well as the transport and perception of auxin between achenes and receptacles (Fig. 6). Leveraging recently available high-quality haplotype-phased reference genomes and genome-wide transcriptome profiling analysis, we were able to unveil the network of genes in auxin homeostasis and enhance our understanding of the regulatory mechanisms during fruit development in strawberry.

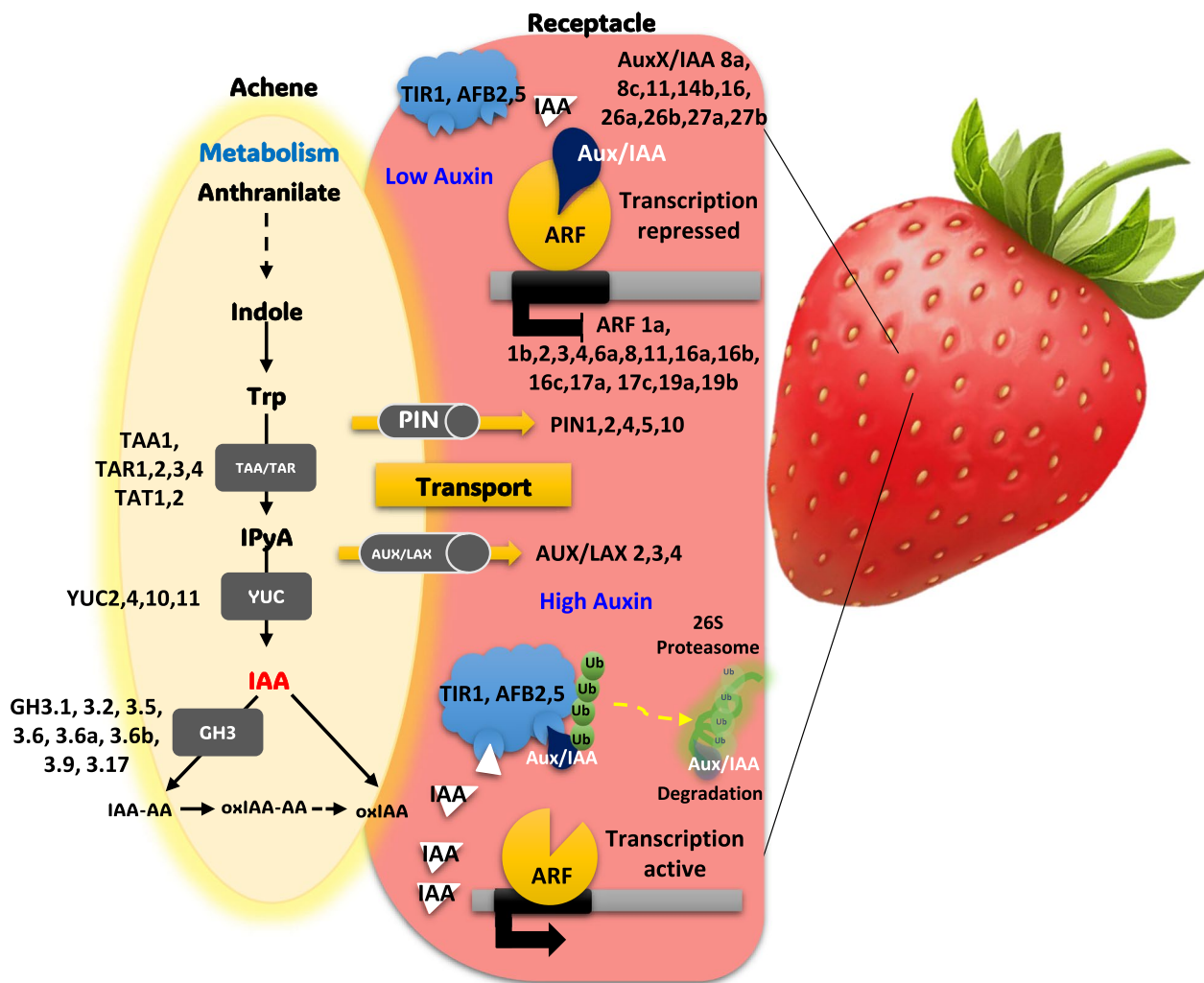


Fig. 6 Model of auxin-related genes transcriptional behavior in achene and receptacle of strawberry fruits. Auxin signaling pathway in strawberry development, highlighting key genetic components. Metabolic processes convert anthranilate to tryptophan, involving genes like TAA1 and TAR1,2, which lead to the production of the hormone auxin (IAA). The transport of auxin is facilitated by PIN and AUX/LAX proteins, crucial for establishing concentration gradients within the plant. In response to auxin levels, the Aux/IAA proteins may regulate gene expression by either repressing or permitting the activity of ARF proteins. High auxin levels trigger the degradation of Aux/IAA repressors, allowing ARF to activate transcription. Genes such as TIR1 and AFB2,5 are essential for auxin perception, initiating the proteasomal degradation pathway

Materials and methods

Sample preparations

The samples of the strawberry fruits (*Fragaria × ananassa* Duch. cv. Brilliance) were used for transcriptome analysis. The six different developmental stages of harvested fruits corresponded that stage 1 is Small Green (SG- The transverse diameter (width) of the strawberry fruit is 1 cm, and the longitudinal diameter (length) is 2 cm), stage 2 is Medium Green (MG- The width of the strawberry fruit expands to 2 cm, distinguishing it from the SG stage, while the length remains 2 cm, similar to the SG stage), stage 3 is Large Green (LG- The width of the strawberry fruit remains 2 cm, but the length increases

to 3 cm, distinguishing it from the MG stage), stage 4 is White (W), stage 5 is Turning Red (TR), and stage 6 is Red (R). In early January, the fruits were harvested from the UF strawberry field at Gulf Coast Research and Education Center in Balm, Florida. All stages of the fruits, including transcriptome sequencing biological replicated, were harvested simultaneously. Using the forceps and scalpels, each stage of the achenes and receptacle were separated from the fruits.

Auxin measurement

Approximately 20 mg (fresh weight) of achene and receptacle samples from 6 fruit stages were immediately frozen

in liquid nitrogen and stored at -80°C . For IAA extraction and purification, frozen samples of achenes and receptacles were ground with pestles in liquid nitrogen and promptly submerged in 1.1 mL sodium phosphate buffer (50 mM, pH 7.0) containing 0.1% diethyl dithiocarbamic acid sodium salt and 10 ng/mL of $[^{13}\text{C}_6]$ -IAA as internal standard. Samples were incubated at 4°C with continuous shaking for 40 min and then centrifuged at 13000 g at 4°C for 15 min. After collecting supernatant and adjusting pH to 2.7, samples were purified by solid-phase extraction using OasisTM HLB columns (WAT094225; Waters, MA, USA). The final elutes with 80% methanol were evaporated to dryness *in vacuo* and stored at -20°C until LC/MS analysis.

Perez et al. (2021) provided the basis for the IAA detection method employed in this study, which utilized liquid chromatography and mass spectrometry (LC–MS) [58]. All samples were resuspended in MilliQ water and analyzed using Vanquish Horizon ultra-high performance liquid chromatography (UHPLC) installed with an Eclipse Plus C18 column (2.1×50 mm, $1.8 \mu\text{m}$) (Agilent) and mass analysis was performed using a TSQ Altis Triple Quadrupole (Thermo Scientific) MS/MS system with an ion funnel. MRM parameters of the standards (precursor m/z , fragment m/z , radio frequency (RF) lens and collision energy) of each compound were optimized on the machine using direct infusion of the authentic standards. IAA and $[^{13}\text{C}_6]$ -IAA were purchased from Cambridge Isotope Laboratories. For IAA detection, the mass spectrometer was operated in positive ionization mode at an ion spray voltage of 4800 V. Formic acid (0.1%) in water and 100% acetonitrile were used as mobile phases A and B, respectively, with a gradient program (0–95% solvent B over 4 min) at a flow rate of 0.4 mL per min. The sheath gas, aux gas and sweep gas were set at 50, 9 and 1 (arbitrary units), respectively. Ion transfer tube temperature and vaporizer temperature were set at 325°C and 350°C , respectively. For MRM monitoring, both Q1 and Q3 resolutions were set at 0.7 FWHM with collision-induced dissociation (CID) gas at 1.5 mTorr. The scan cycle time was 0.8 s. MRM for IAA was used to monitor parent ion \rightarrow product ion reactions for each analyte as follows: m/z 175.983 \rightarrow 130.071 (CE, 18 V) for IAA; m/z 182.091 \rightarrow 136 (CE, 18 V) for $[^{13}\text{C}_6]$ -IAA. IAA analysis was conducted with three biological replicates.

Transcriptome data analysis

The total RNA from separate achene and receptacle at six development stage with three replications per sample were extracted by the SpectrumTM Plant Total RNA Kit (Sigma-Aldrich, MO, USA) as following the manufacturer protocol. To generate RNA-seq for illumina

sequencing library were followed Illumina sequencing protocol. The resulting sequencing library were performed pair-end sequenced (2×150 bp) by Illumina NovaSeq instruments at Novogene Bioinformatics Institute, Beijing, China. Raw read sequences obtained from 36 sequenced libraries were quality trimmed and filtered using Trimmomatic [59]. Data quality was assessed using FastQC. Trimmed paired end reads were aligned to the ‘Royal Royce’ octoploid genome [31] using Hisat2 [60]. Differentially expressed genes (DEG) analysis was conducted using the DESeq2 package in R script [61] using a $\text{padj} < 0.05$ (after the false discovery rate adjustment for multiple testing ($\text{FDR} < 0.05$) for the null hypothesis. Total number of reads mapped to each gene was used to calculate transcripts per million (TPM) values, which were determined using a custom Python script. Gene Ontology (GO) enrichment analysis was conducted using Arabidopsis gene information provided by the Royal Royce genome annotation database [31]. The analysis was conducted through the ShinyGO tool (version 0.77, <http://bioinformatics.sdstate.edu/go/>, [62]), applying a P-value cutoff of ≤ 0.05 (FDR) and default options.

Confirmation of homology of octoploid strawberry auxin hormone pathway genes

Genes associated with auxin biosynthesis were explored in the octoploid strawberry involved utilizing known genes from *F. vesca* and previous literature [11, 28, 63]. BlastP was performed with significant criteria under $e\text{-value} = 0$, $\text{pident} < 90$, $\text{bit score} > 100$ based on the protein sequence against the Royal Royce reference genome [31] for each hormone-related gene.

K-means clustering and gene co-expression analysis

Transcripts per million (TPM) counts were used as input for the K-means clustering analysis. TPM values were averaged for the replicates of each tissue (achene or receptacle) at any given stage (Stage 1 to Stage 6). Averaged TPM values were normalized to $\log_2(\text{TPM} + 1)$, scaled, and used as input for clustering analysis. DEGs were categorized into four clusters using the k-means algorithm implemented using the R programming language. In order to identify transcriptional correlations among genes with shared expression profile analysis achene or receptacle, the *cor* function was implemented in the R package WGCNA. Then, genes with shared expression profiles were considered as seed candidates and were used to build a gene co-expression analysis to obtain direct and indirect interactions. A high confidence score of 0.7 was used as a threshold [64]. Only high levels of confidence interactions were considered as valid as used in the final gene co-expression analysis.

Validation of auxin related gene expression by qRT-PCR analysis

To validate auxin-related genes, total RNA (1 µg) was treated with Deoxyribonuclease I (DNase I) (Invitrogen, Carlsbad, CA) to remove residual DNA prior to cDNA synthesis, following the manufacturer's instructions. The DNase I-treated RNA was reverse transcribed using oligo(dT) primers and M-MLV reverse transcriptase (M0253, New England BioLabs). Quantitative PCR was conducted using the FastStart Essential master mix (Roche Applied Science) in accordance with the manufacturer's protocol. Each qRT-PCR reaction consisted of 10 µL of the PCR pre-mix, 4 µL of cDNA, and 500 nM of each primer, except for *FaGAPDH* where 250 nM of each primer was used. Gene-specific primers were designed with the Primer3 software [65] (Supplemental Table 8), utilizing default settings. The PCR conditions were: initial denaturation at 95°C for 10 min, followed by 40 cycles at 95°C for 10 s, annealing at 60°C for 10 s, and extension at 72°C for 10 s. Relative gene expression was calculated using the ΔC_q method (quantification cycle (C_q) value of the target gene minus C_q of *FaGAPDH*) and log fold change was determined using the $2^{-\Delta\Delta C_q}$ method.

Abbreviations

ABA	Abscissic Acid
AP2/ERF	Apetala2/Ethylene Responsive Factor
ARFs	Auxin Response Factor
Aux/IAAs	Auxin/Indole-3-Acetic Acid Proteins
bZIP	Basic Region/ Leucine Zipper Motif
BP	Biological Process
CC	Cell Components
GO	Gene Ontology
GH3s	Gretchen Hagen 3
IAA	Indole-3-Acetic Acid
IPyA	Indole-3-Pyruvic Acid
KEGG	Kyoto Encyclopedia Of Genes And Genomes
LG	Large Green
MG	Medium Green
MF	Molecular Functions
NAC/WYKY	NAM-ATAF1,2-CUC2/ WRKYGQK motif ()
PAA	Phenylacetic Acid
PINs	Pin-Formed
PCA	Principal Component Analysis
R	Red
FaRR1	Royal Royce
SG	Small Green
TAR	Taa-Related
TIR1	Transport Inhibitor Response 1
TIR/AFBs	Transport Inhibitor Response 1 / Auxin-Signaling F-Box
TAA	Tryptophan Aminotransferase Of Arabidopsis
TR	Turning Red
W	White
YUCs	YUCCA

Supplementary Information

The online version contains supplementary material available at <https://doi.org/10.1186/s12870-024-05577-5>.

Supplementary Material 1.

Supplementary Material 2.

Supplementary Material 3.

Supplementary Material 4.

Supplementary Material 5.

Supplementary Material 6.

Supplementary Material 7.

Supplementary Material 8.

Acknowledgements

We extend our gratitude to Dr. Vance M. Whitaker for providing the fruit materials used in this study. The authors thank for the technical support and assistance with fruit preparations provided by Dr. Youngjae Oh and Sadikshya Sharma. Also, we thank Ru Dai and Veronica Perez for their technical support for auxin quantification.

Authors' contributions

YJ, KB, JK and SL contributed to the study design and drafted the article. YJ, JK, TK, KB, HH, ML, ZL, VW, SL and analyzed the experiment results, prepared figures and tables. All authors read and approved the manuscript.

Funding

This research is supported by grants from the United States Department of Agriculture National Institute of Food and Agriculture (NIFA) Specialty Crops Research Initiative (SCRI) "Delivering Breeding and Management Solutions to Prevent Losses to Emerging and Expanding Disease Threats in Strawberry" under award number (#2022-51181-38328) and NSF-IOS-CAREER-2142898.

Availability of data and materials

High-throughput sequencing data analyzed in present study are available under NCBI BioProject PRJNA1010111. The online version contains Supporting Information available.

Declarations

Ethics approval and consent to participate

Not applicable.

Consent for publication

Not applicable.

Competing interests

The authors declare no competing interests.

Author details

¹Gulf Coast Research and Education Center, Institute of Food and Agricultural Science, University of Florida, Wimauma, FL 33598, USA. ²Horticultural Sciences Department, University of Florida, Gainesville, FL 32611, USA. ³Plant Molecular and Cellular Biology Graduate Program, University of Florida, Gainesville, FL 32611, USA. ⁴Environmental Horticulture Department, University of Florida, Gainesville, FL 32611, USA. ⁵Department of Cell Biology and Molecular Genetics, University of Maryland, College Park, MD 20742, USA.

Received: 16 June 2024 Accepted: 9 September 2024

Published online: 20 September 2024

References

- Hardigan MA, Feldmann MJ, Lorant A, Bird KA, Famula R, Acharya C, Cole G, Edger PP, Knapp SJ. Genome synteny has been conserved among the octoploid progenitors of cultivated strawberry over millions of years of evolution. *Front Plant Sci.* 2020;10:1789.
- Edger PP, Poorten TJ, VanBuren R, Hardigan MA, Colle M, McKain MR, Smith RD, Teresi SJ, Nelson AD, Wai CM. Origin and evolution of the octoploid strawberry genome. *Nat Genet.* 2019;51(3):541–7.
- Liu Z, Ma H, Jung S, Main D, Guo L. Developmental mechanisms of fleshy fruit diversity in Rosaceae. *Annu Rev Plant Biol.* 2020;71:547–73.

4. Xiang Y, Huang C-H, Hu Y, Wen J, Li S, Yi T, Chen H, Xiang J, Ma H. Evolution of Rosaceae fruit types based on nuclear phylogeny in the context of geological times and genome duplication. *Mol Biol Evol*. 2017;34(2):262–81.
5. Veerappan K, Natarajan S, Chung H, Park J. Molecular insights of fruit quality traits in peaches, *Prunus persica*. *Plants*. 2021;10(10):2191.
6. Tian Y, Xin W, Lin J, Ma J, He J, Wang X, Xu T, Tang W. Auxin Coordinates Achene and Receptacle Development During Fruit Initiation in *Fragaria vesca*. *Front Plant Sci*. 2022;13:929831.
7. Guo L, Luo X, Li M, Joldersma D, Plunkert M, Liu Z. Mechanism of fertilization-induced auxin synthesis in the endosperm for seed and fruit development. *Nat Commun*. 2022;13(1):1–15.
8. Perkins-Veazie P. Growth and Ripening of Strawberry Fruit. In: *Horticultural Reviews*. 1995. p. 267–97.
9. Gu Q, Ferrándiz C, Yanofsky MF, Martienssen R. The FRUITFULL MADS-box gene mediates cell differentiation during Arabidopsis fruit development. *Development*. 1998;125(8):1509–17.
10. Gorguet B, Van Heusden A, Lindhout P. Parthenocarpic fruit development in tomato. *Plant Biol*. 2005;7(02):131–9.
11. Kang C, Darwish O, Geretz A, Shahar N, Alkharouf N, Liu Z. Genome-scale transcriptomic insights into early-stage fruit development in woodland strawberry *Fragaria vesca*. *Plant Cell*. 2013;25(6):1960–78.
12. Galimba KD, Bullock DG, Dardick C, Liu Z, Callahan AM. Gibberellic acid induced parthenocarpic 'Honeycrisp' apples (*Malus domestica*) exhibit reduced ovary width and lower acidity. *Hortic Res*. 2019;6:41.
13. Pattison RJ, Catalá C. Evaluating auxin distribution in tomato (*Solanum lycopersicum*) through an analysis of the PIN and AUX/LAX gene families. *Plant J*. 2012;70(4):585–98.
14. Vivian-Smith A, Luo M, Chaudhury A, Koltunow A. Fruit development is actively restricted in the absence of fertilization in Arabidopsis. *Development*. 2001;128:2321–31.
15. Katel S, Mandal HR, Kattel S, Yadav SPS, Lamshaj BS. Impacts of plant growth regulators in strawberry plant: A review. *Heliyon*. 2022;8(12):e11959.
16. Li L, Li D, Luo Z, Huang X, Li X. Proteomic response and quality maintenance in postharvest fruit of strawberry (*Fragaria x ananassa*) to exogenous cytokinin. *Sci Rep*. 2016;6(1):27094.
17. Liao X, Li M, Liu B, Yan M, Yu X, Zi H, Liu R, Yamamoto C. Interlinked regulatory loops of ABA catabolism and biosynthesis coordinate fruit growth and ripening in woodland strawberry. *Proc Natl Acad Sci U S A*. 2018;115(49):E11542–50.
18. Feng J, Dai C, Luo H, Han Y, Liu Z, Kang C. Reporter gene expression reveals precise auxin synthesis sites during fruit and root development in wild strawberry. *J Exp Bot*. 2019;70(2):563–74.
19. Woodward AW, Bartel B. Auxin: regulation, action, and interaction. *Ann Bot*. 2005;95(5):707–35.
20. Mashiguchi K, Tanaka K, Sakai T, Sugawara S, Kawaide H, Natsume M, Hanada A, Yaeno T, Shirasu K, Yao H. The main auxin biosynthesis pathway in Arabidopsis. *Proc Natl Acad Sci U S A*. 2011;108(45):18512–7.
21. Given NK, Venis MA, Gierson D. Hormonal regulation of ripening in the strawberry, a non-climacteric fruit. *Planta*. 1988;174(3):402–6.
22. Nitsch J. Free Auxins and Free Tryptophan in the Strawberry. *Plant Physiol*. 1955;30(1):33.
23. Nitsch J. Growth and morphogenesis of the strawberry as related to auxin. *Am J Botany*. 1950;37(3):211–5.
24. Nitsch J. Plant hormones in the development of fruits. *Q Rev Biol*. 1952;27(1):33–57.
25. Won C, Shen X, Mashiguchi K, Zheng Z, Dai X, Cheng Y, Kasahara H, Kamiya Y, Chory J, Zhao Y. Conversion of tryptophan to indole-3-acetic acid by TRYPTOPHAN AMINOTRANSFERASES OF ARABIDOPSIS and YUCCAs in Arabidopsis. *Proc Natl Acad Sci U S A*. 2011;108(45):18518–23.
26. Liu H, Xie WF, Zhang L, Valpuesta V, Ye ZW, Gao QH, Duan K. Auxin biosynthesis by the YUCCA6 flavin monooxygenase gene in woodland strawberry. *J Integr Plant Biol*. 2014;56(4):350–63.
27. Liu H, Ying Y-Y, Zhang L, Gao Q-H, Li J, Zhang Z, Fang J-G, Duan K. Isolation and characterization of two YUCCA flavin monooxygenase genes from cultivated strawberry (*Fragaria x ananassa* Duch.). *Plant Cell Rep*. 2012;31:1425–35.
28. Estrada-Johnson E, Csukasi F, Pizarro CM, Vallarino JG, Kiryakova Y, Vioque A, Brumos J, Medina-Escobar N, Botella MA, Alonso JM. Transcriptomic analysis in strawberry fruits reveals active auxin biosynthesis and signaling in the ripe receptacle. *Front Plant Sci*. 2017;8:889.
29. Dharmasiri N, Dharmasiri S, Estelle M. The F-box protein TIR1 is an auxin receptor. *Nature*. 2005;435(7041):441–5.
30. Calderón Villalobos LIA, Lee S, De Oliveira C, Ivetac A, Brandt W, Armitage L, Sheard LB, Tan X, Parry G, Mao H. A combinatorial TIR1/AFB-Aux/IAA co-receptor system for differential sensing of auxin. *Nat Chem Biol*. 2012;8(5):477–85.
31. Hardigan MA, Feldmann MJ, Pincot DD, Famula RA, Vachev MV, Madera MA, Zerbe P, Mars K, Peluso P, Rank D. Blueprint for phasing and assembling the genomes of heterozygous polyploids: application to the octoploid genome of strawberry. *BioRxiv*. 2021;2003:467115.
32. Wang H, Tian C-e, Duan J, Wu K. Research progresses on GH3s, one family of primary auxin-responsive genes. *Plant Growth Regul*. 2008;56:225–32.
33. Vaddepalli P, de Zeeuw T, Strauss S, Bürstenbinder K, Liao C-Y, Ramalho JJ, Smith RS, Weijers D. Auxin-dependent control of cytoskeleton and cell shape regulates division orientation in the Arabidopsis embryo. *Curr Biol*. 2021;31(22):4946–4955.e4944.
34. Petersson SV, Johansson AI, Kowalczyk M, Makoveychuk A, Wang JY, Moritz T, Grebe M, Benfey PN, Sandberg G, Ljung K. An auxin gradient and maximum in the Arabidopsis root apex shown by high-resolution cell-specific analysis of IAA distribution and synthesis. *Plant Cell*. 2009;21(6):1659–68.
35. Alabadí D, Blázquez MA, Carbonell J, Ferrándiz C, Pérez-Amador MA. Instructive roles for hormones in plant development. *Int J Dev Biol*. 2009;53(8):1597.
36. Sánchez-Sevilla JF, Vallarino JG, Osorio S, Bombarely A, Posé D, Merchante C, Botella MA, Amaya I, Valpuesta V. Gene expression atlas of fruit ripening and transcriptome assembly from RNA-seq data in octoploid strawberry (*Fragaria x ananassa*). *Sci Rep*. 2017;7(1):1–13.
37. Symons G, Chua Y-J, Ross J, Quittenden L, Davies N, Reid J. Hormonal changes during non-climacteric ripening in strawberry. *J Exp Bot*. 2012;63(13):4741–50.
38. Gu T, Jia S, Huang X, Wang L, Fu W, Huo G, Gan L, Ding J, Li Y. Transcriptome and hormone analyses provide insights into hormonal regulation in strawberry ripening. *Planta*. 2019;250(1):145–62.
39. Liu D-j, Chen J-y, Lu W-j. Expression and regulation of the early auxin-responsive Aux/IAA genes during strawberry fruit development. *Mol Biol Rep*. 2011;38:1187–93.
40. Luo P, Di D-W. Precise regulation of the TAA1/TAR-YUCCA auxin biosynthesis pathway in plants. *Int J Mol Sci*. 2023;24(10):8514.
41. Lu R, Pi M, Liu Z, Kang C. Auxin biosynthesis gene FveYUC4 is critical for leaf and flower morphogenesis in woodland strawberry. *Plant J*. 2023;115(5):1428–42.
42. Archbold D, Dennis F. Quantification of free ABA and free and conjugated IAA in strawberry achene and receptacle tissue during fruit development. *J Am Soc Hortic Sci*. 1984;109(3):330–5.
43. Park S, Cohen JD, Slovin JP. Strawberry fruit protein with a novel indole-acyl modification. *Planta*. 2006;224:1015–22.
44. Fukui K, Arai K, Tanaka Y, Aoi Y, Kukshal V, Jez JM, Kubes MF, Napier R, Zhao Y, Kasahara H. Chemical inhibition of the auxin inactivation pathway uncovers the roles of metabolic turnover in auxin homeostasis. *Proc Natl Acad Sci*. 2022;119(32):e2206869119.
45. Petrásěk J, Mravec J, Bouchard R, Blakeslee JJ, Abas M, Seifertová D, Wisniewska J, Tadele Z, Kubes M, Covanová M. PIN proteins perform a rate-limiting function in cellular auxin efflux. *Science*. 2006;312(5775):914–8.
46. Adamowski M, Friml J. PIN-dependent auxin transport: action, regulation, and evolution. *Plant Cell*. 2015;27(1):20–32.
47. Liscum E, Reed J. Genetics of Aux/IAA and ARF action in plant growth and development. *Plant Mol Biol*. 2002;49:387–400.
48. Devoghalere F, Doucen T, Guittion B, Keeling J, Payne W, Ling TJ, Ross JJ, Hallett IC, Gunaseelan K, Dayatilake G. A genomics approach to understanding the role of auxin in apple (*Malus x domestica*) fruit size control. *BMC Plant Biol*. 2012;12:1–15.
49. Weijers D, Wagner D. Transcriptional responses to the auxin hormone. *Annu Rev Plant Biol*. 2016;67:539–74.
50. Schaffer RJ, Ireland HS, Ross JJ, Ling TJ, David KM. SEPALLATA1/2-suppressed mature apples have low ethylene, high auxin and reduced transcription of ripening-related genes. *AOB plants*. 2013;5:pls047.

51. LeClere S, Schmelz EA, Chourey PS. Sugar levels regulate tryptophan-dependent auxin biosynthesis in developing maize kernels. *Plant Physiol.* 2010;153(1):306–18.
52. Stepanova AN, Robertson-Hoyt J, Yun J, Benavente LM, Xie D-Y, Doležal K, Schlereth A, Jürgens G, Alonso JM. TAA1-mediated auxin biosynthesis is essential for hormone crosstalk and plant development. *Cell.* 2008;133(1):177–91.
53. Expósito-Rodríguez M, Borges AA, Borges-Pérez A, Pérez JA. Gene structure and spatiotemporal expression profile of tomato genes encoding YUCCA-like flavin monooxygenases: the ToFZY gene family. *Plant Physiol Biochem.* 2011;49(7):782–91.
54. Tivendale ND, Davidson SE, Davies NW, Smith JA, Dalmais M, Bendahmane AI, Quittenden LJ, Sutton L, Bala RK, Le Signor C. Biosynthesis of the halogenated auxin, 4-chloroindole-3-acetic acid. *Plant Physiol.* 2012;159(3):1055–63.
55. Reinecke DM. 4-Chloroindole-3-acetic acid and plant growth. *Plant Growth Regul.* 1999;27:3–13.
56. Carrasco-Orellana C, Stappung Y, Mendez-Yañez A, Allan A, Espley R, Plunkett B, Moya-Leon M, Herrera R. Characterization of a ripening-related transcription factor FcNAC1 from *Fragaria chiloensis* fruit. *Sci Rep.* 2018;8(1):10524.
57. El-Sharkawy I, Sherif S, Qubbaj T, Sullivan AJ, Jayasankar S. Stimulated auxin levels enhance plum fruit ripening, but limit shelf-life characteristics. *Postharvest Biol Technol.* 2016;112:215–23.
58. Perez VC, Dai R, Bai B, Tomiczek B, Askey BC, Zhang Y, Rubin GM, Ding Y, Grenning A, Block AK. Aldoximes are precursors of auxins in *Arabidopsis* and maize. *New Phytol.* 2021;231(4):1449–61.
59. Bolger AM, Lohse M, Usadel B. Trimmomatic: a flexible trimmer for Illumina sequence data. *Bioinformatics.* 2014;30(15):2114–20.
60. Kim D, Paggi JM, Park C, Bennett C, Salzberg SL. Graph-based genome alignment and genotyping with HISAT2 and HISAT-genotype. *Nat Biotechnol.* 2019;37(8):907–15.
61. Love M, Anders S, Huber W. Differential analysis of count data—the DESeq2 package. *Genome Biol.* 2014;15(550):10–1186.
62. Ge SX, Jung D, Yao R. ShinyGO: a graphical gene-set enrichment tool for animals and plants. *Bioinformatics.* 2020;36(8):2628–9.
63. Li Y, Pi M, Gao Q, Liu Z, Kang C. Updated annotation of the wild strawberry *Fragaria vesca* V4 genome. *Hort Res.* 2019;6:61.
64. Begcy K, Nosenko T, Zhou L-Z, Fagner L, Weckwerth W, Dresselhaus T. Male sterility in maize after transient heat stress during the tetrad stage of pollen development. *Plant Physiol.* 2019;181(2):683–700.
65. Untergasser A, Cutcutache I, Koressaar T, Ye J, Faircloth BC, Remm M, Rozen SG. Primer3—new capabilities and interfaces. *Nucleic Acids Res.* 2012;40(15):e115–e115.

Publisher's Note

Springer Nature remains neutral with regard to jurisdictional claims in published maps and institutional affiliations.